

## **Fe<sub>3</sub>O<sub>4</sub>@SiO<sub>2</sub>@IL-PVP magnetic nanoparticles: Effective synthesis of spirooxindoles**

**Shahla Veysipour, Masoud Nasr-Esfahani\*, Zahra Rafiee, Behrouz Eftekhari far**

*Department of Chemistry, Faculty of Science, Yasouj University, Yasouj, 75918-74831, Iran.*

Received 3 March 2020; received in revised form 23 May 2021; accepted 25 May 2021

### ABSTRACT

Various magnetite heterogeneous catalysts for the organic reaction are increasingly recognized while their stability still is a critical challenge. In this regard, SiO<sub>2</sub>, ionic liquid (IL), and polyvinyl pyrrolidone (PVP) were applied as a three-layer stabilization system for modifying magnetic Fe<sub>3</sub>O<sub>4</sub> to produce Fe<sub>3</sub>O<sub>4</sub>@SiO<sub>2</sub>@IL-PVP as a novel nanocatalyst. The Fe<sub>3</sub>O<sub>4</sub>@SiO<sub>2</sub>@IL-PVP as stabilized heterogeneous catalysts were utilized in a robust, and environmentally friendly strategy for the preparation of the spirooxindole derivatives by the one-pot condensation of isatin, malononitrile, and 1,3-dicarbonyl in a water solvent. The proposed method revealed a high yield spirooxindole derivatives preparation (99%) at short reaction times (1.0 min), low catalyst mass (0.002 g), and satisfactory temperature (30 °C) which confirm the lack of any tedious challenge and promising applicability and reusability. This work introduces a rational core-shell nanosystem design with a facile and novel construction strategy to arrive at nonexquisite metal-based composite catalysts with superior catalytic proficiency and prominent long-term stability.

**Keywords:** *Magnetic nanoparticles, Spirooxindoles, Green synthesis, Fe<sub>3</sub>O<sub>4</sub>@SiO<sub>2</sub>@IL-PVP nanocomposite, Reusable catalyst.*

### 1. Introduction

Recently, heterogeneous catalysts attracted much attention to researchers due to the fact that they possess a lesser amount of problems than homogeneous catalysts, for example, challenges in the filtration of the desired products and catalyst particles separation from liquid upon reaction completion [1-3]. To overcome these drawbacks, nanoparticles as alternative support for heterogeneous catalysis have been used to combine the benefits of both homogeneous and heterogeneous catalysts [4,5]. Since the comfortable and quick separation and collection of the catalyst from the reaction media is a vital parameter in catalytic-based reactions, while, isolation and reuse of catalysts has some problems. In this regard, the magnetite (Fe<sub>3</sub>O<sub>4</sub>) supported nanocatalyst has proven to be rapidly and effortlessly separated and collected from the reaction mixture using an outside magnetic force [6-10].

In recent decades, the development and expansion of magnetic nanoparticles (MNPs) has achieved much consideration due to their important properties such as desirable magnetic and electrical characters, medium surface area, their unrivaled catalytic performance, and their extensive uses in the green chemistry scope because of the environmentally benign temperament of these materials [11]. But pure NPs of iron oxides always join to accumulate due to anisotropic dipolar and strong interaction between each other (12). It is shown that magnetic nanoparticles are usually coated with organic or inorganic shells to improve their chemical stability and prevent their accumulation in liquids media (10). Organic coatings can include natural polymers such as starch [13], gelatin [14], dextran [15], chitosan [16] and synthetic polymers such as polyethylene glycol [17], polyvinyl alcohol [18], polyacrylic acid [19] and polyvinyl pyrrolidone [20]. Generally, inorganic coatings are metal oxides, precious metals, and silica [21]. At present, considerably has been engrossed on composites of the magnetic core-shell structure as catalysts through the coating of a silica shell around the

\*Corresponding author.

E-mail address: *manas@yu.ac.ir; m\_nasr\_e@yahoo.com*  
(M. Nasr Esfahani)

performed iron oxide NPs has attracted much attestation [22]. Besides, the intelligent design and blend of polymers, magnetite nanoclusters and ionic liquids (ILs) offer a new and special feature of polymer immobilized on magnetic nanoparticles modified by an ionic liquid with desirable properties. Multi-component reactions (MCRs) possess importance as a robust and capable strategy in organic synthesis due to their numerous applications, especially in the production of biologically active materials that precede a vital research field in organic and phytochemistry. Some of the advantages of this method are the construction of complex and supramolecular organic materials from simple and easily accessible raw material which is able to receive in a quick and impressive procedure devoid of the isolation of any intermediate and also procedural simplicity, inherent atom economy, facile workup, and environmental friendliness [23-26].

Spirooxindoles as heterocyclic compounds combined cyclic structures fused at a central C atom have recently been of considerable interest due to their existence both in nature and in a biologically active molecule [11]. These materials revealed a broad range of useful biological and pharmaceutical applications such as antitumor [27], antimalarial [28], antiviral [29], antifungal [30], antibacterial, anti-inflammatory, antipyretic [31], anti-HIV [32], anti-tubercular [33], anti-microbial [34] activities. One-pot, three-component reaction of isatin, cyclic 1,3-dicarbonyl compounds and malononitrile is the most appropriate strategy for the synthesis of these compounds. Recently, spirooxindole derivatives have been prepared in the presence of the average performance catalysts such as  $\text{InCl}_3$  [35], tetra-*n*-butylammonium fluoride (TBAF) [36],  $\beta$ -cyclodextrin [37],  $\text{NH}_4\text{Cl}$  [38], triethylbenzylammonium chloride (TEBA) [39], ethylenediamine diacetate (EDDA) [40], Sodium stearate [41], SBA-Pr-NH<sub>2</sub> [42], (SB-DBU)Cl [43], citric acid [44],  $\text{Fe}_3\text{O}_4@/\text{SiO}_2$ -imid-PMA [45]. However, some of the reported methods succumb to drastic reaction conditions, medium yields, extended reaction time, consumption of large amounts of catalyst, use of toxic catalyst, and challenge in separation, collection and durability of the catalyst. The development of an advanced catalytic-based system to overcome these constraints for the synthesis of spirooxindole derivatives is still desirable and favored. Hence, we used comprehensively polyvinylpyrrolidone (PVP) immobilized  $\text{Fe}_3\text{O}_4@/\text{SiO}_2@/\text{IL}$  as a durable catalyst for the three-component and one-pot preparation of amidoalkyl naphthols [46]. Compared to other report catalyst support (metal-organic frameworks, ion-exchange resins, carbon-based materials, and nano-

tania),  $\text{Fe}_3\text{O}_4@/\text{SiO}_2@/\text{IL-PVP}$  possesses several advantages including prominent loading capacity, desirable chemical stability, and capable recoverability. **Scheme 1** illustrates the steps for the construction of  $\text{Fe}_3\text{O}_4@/\text{SiO}_2@/\text{IL-PVP}$  nanocatalyst.

## 2. Experimental

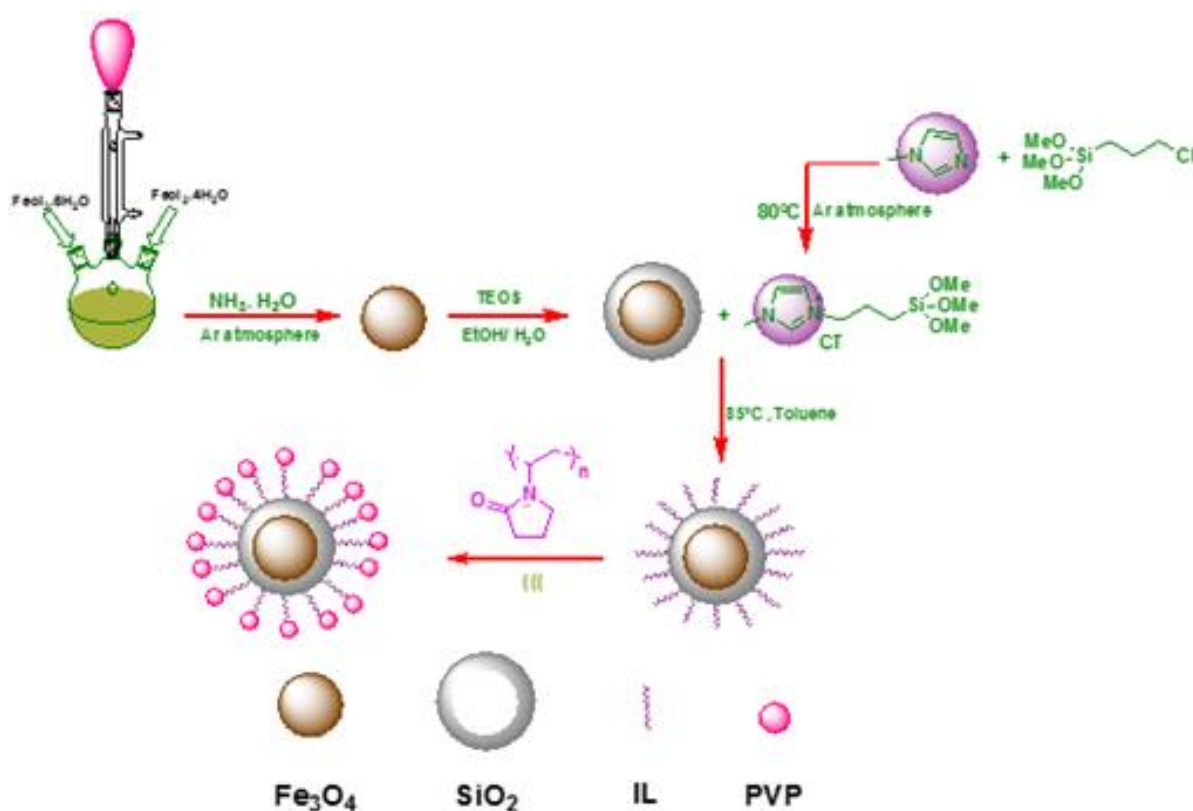
### 2.1. Chemicals and instrumentation

All chemicals were commercially obtained from Merck and Sigma Aldrich and used without additional purification. Melting points were measured using an Electrothermal KSBIN device. Product purity and reaction monitoring were performed using thin-film chromatography (TLC) on PolyGram SILG/UV 254 silica gel plates. Fourier transform infrared (FT-IR) spectroscopy were recorded in the range of 400-4000  $\text{cm}^{-1}$  on a JASCO FT-IR/680 spectrophotometers.  $^1\text{H}$  NMR and  $^{13}\text{C}$  NMR spectra were determined at 400 and 100 MHz on Bruker Avance UltraShield 400 MHz instrument spectrometer, respectively, which DMSO-*d*<sub>6</sub> and tetramethylsilane (TMS) were applied as a solvent and internal standard, respectively. Scanning electron microscopy (SEM) equipped with an EDX Sirius SD detector was applied to the morphology and elemental composition of the samples. The particle size distribution and precise morphology of the prepared samples were studied by transmitting electron microscopy (TEM) under the Zeiss EM10C microscope at 100 kV. X-ray powder diffraction (XRD) patterns were used to determine the crystallites of samples prepared by a Bruker AXS (D8 Advance) X-ray diffractometer with Cu K $\alpha$  radiation ( $\lambda = 0.15418$  nm). The magnetic properties measurement (vibrating-sample magnetometer; VSM) was obtained using a VSM LKBFB Model-Meghnatis Daghigh Kavir Company. Thermal gravimetric analysis (TGA) was obtained under a nitrogen atmosphere using the STA 6000, Perkin Elmer apparatus at a heating rate of 20  $^\circ\text{C}/\text{min}$  and in the temperature range of 30-800  $^\circ\text{C}$  for 5 mg of each sample.

### 2.2. Catalyst preparation

#### 2.2.1. Preparation of $\text{Fe}_3\text{O}_4@/\text{SiO}_2$ nanoparticles

The core-shell  $\text{Fe}_3\text{O}_4@/\text{SiO}_2$  nanospheres were carried out using a manner similar to the method used in our previous reports [46]. In a typical procedure,  $\text{FeCl}_3 \cdot 6\text{H}_2\text{O}$  (10 mmol, 2.7 g) and  $\text{FeCl}_2 \cdot 4\text{H}_2\text{O}$  (5 mmol, 1 g) were added to the reaction vessel containing 50 ml double-distilled water, was then mechanically stirred at 80  $^\circ\text{C}$  for 30 min, under an argon atmosphere. Then, the



**Scheme 1.** Synthesis of magnetic silica nanoparticles modified by ionic liquids and immobilization of polyvinyl pyrrolidone (PVP)

$\text{NH}_4\text{OH}$  solution (25%, 10 ml) was slowly added to the mixture with vigorous stirring. After stirring the mixture for 1 hour under argon atmosphere at 80 °C, the prepared  $\text{Fe}_3\text{O}_4$  nanoparticles were separated from the reaction vessel using an external magnetic field and washed several times with deionized water to remove the remaining impurities and the product was dried for 10 h at 60 °C. To prepared silica-coated iron oxide magnetic nanoparticles, (0.50 g)  $\text{Fe}_3\text{O}_4$  magnetic nanoparticles were added to a mixture of ethanol (80 ml) and deionized water (20 ml) and the mixture was dispersed in ultrasonic bath for 15 min, then to the mixture reaction 3.0 ml of 28 wt% concentrated ammonia aqueous solution, followed by the slow addition of 0.5 ml of TEOS (tetraethylorthosilicate). The mixture was stirred for 24 h under reflux conditions with a magnetic stirrer and finally the  $\text{Fe}_3\text{O}_4$  ( $\text{Fe}_3\text{O}_4 @ \text{SiO}_2$ ) coated with silica was separated by an external magnet. The prepared solid was washed with distilled water and dried for 10 hours at 80 °C.

### 2.2.2. Preparation of 1-methyl-3-(3-trimethoxysilylpropyl)-1H-imidazole-3-iumchloride (IL)

For this purpose, in the absence of any catalyst, a mixture of (3-chloropropyl) trimethoxy silane (15.86 mmol, 3.82 ml) and 1-methyl imidazole (15.86 mmol, 1.26 ml) was refluxed for three days in the solvent-free condition under Ar atmosphere at 80 °C. The yellow viscous liquid prepared was washed with diethyl ether (3×5 ml) to remove non-reactive materials. The product was dried under a vacuum [47].

### 2.2.3. Preparation of 1-methyl-3-(3-trimethoxysilylpropyl)-1H-imidazole-3-iumchloride functionalized magnetic nanoparticles ( $\text{Fe}_3\text{O}_4 @ \text{SiO}_2 @ \text{IL}$ )

$\text{Fe}_3\text{O}_4 @ \text{SiO}_2 @ \text{IL}$  magnetic nanoparticles have been prepared according to our previous reports, which is a one-step and easy method [46]. In this method,  $\text{Fe}_3\text{O}_4 @ \text{SiO}_2$  magnetic nanoparticles (0.1 g) were dispersed by ultrasonication in dry toluene (20 ml) for 10 min. Then, 1 g of the as-prepared ionic liquid was added and the solution was stirred for 24 h at 85°C under reflux condition argon atmosphere. In the following, the product reaction ( $\text{Fe}_3\text{O}_4 @ \text{SiO}_2 @ \text{IL}$ ) was detached by an external magnet, washed several times with ethanol and acetonitrile, and then dried in the vacuum oven at 60°C.

#### 2.2.4. Preparation of polyvinyl pyrrolidone (PVP) immobilized magnetic nanoparticles ( $Fe_3O_4@SiO_2@IL-PVP$ )

**Scheme 1** represents the immobilization of PVP onto  $Fe_3O_4@SiO_2@IL$ . 0.25 g of polyvinyl pyrrolidone was added to 20 ml of ethanol in a beaker and dispersed in the mixture for 30 minutes by ultrasonic. Then, 0.1 g of ( $Fe_3O_4@SiO_2@IL$ ) nanoparticles were added to the reaction mixture. The prepared mixture was sonicated for 4 hours and then the prepared magnetic solid was isolated by the simple magnet and washed with ethanol. Finally, the product PVP impregnated  $Fe_3O_4@SiO_2@IL$  was dried at 60 °C under vacuum.

#### 2.2.5. General method for the preparation of spirooxindoles

To a 50 mL round-bottomed flask containing 3 ml distilled water as a solvent, a mixture of isatin (1 mmol), malononitrile (1 mmol), 1,3-dicarbonyl compounds (1 mmol), and  $Fe_3O_4@SiO_2@IL-PVP$  nanoparticles (0.01 g) was added. The reaction mixture was vigorously stirred at 50 °C for the appropriate times as shown in **Table 2**. The reactions progress was controlled by TLC (n-hexane/ethyl acetate, 4:1 ratio). After completion, the reaction mixture was cooled to room temperature. The obtained content was filtered for separation of product and catalyst from water, then washed with 20 ml distilled water and subsequently with 5ml cold ethanol. The remaining solid was dissolved in 10 ml hot ethanol to separate the catalyst by using a simple magnet. The solvent was evaporated, and the pure product was obtained by recrystallization from ethanol (**Scheme 2**).

#### 2-Amino-2',5-dioxo-5,6,7,8-tetrahydrospiro[chromene-4,3'-indoline]-3-carbonitrile (4a)

M.P: 301-302°C (Lit. [48]. 298-299 °C); FT-IR (KBr,  $cm^{-1}$ ): 3349, 3295, 3176, 2950, 2195, 1710, 1685, 1608, 1463, 1351, 1216, 1076, 1012, 935  $cm^{-1}$ .  $^1H$  NMR (400 MHz, DMSO- $d_6$ ):  $\delta$ (ppm)= 10.41 (s, 1H, NH), 7.23 (s, 2H, NH<sub>2</sub>), 7.09-7.17 (m, 1H, aromatic CH), 6.99 (d, 1H,  $J=7.2$  Hz, aromatic CH), 6.90 (t, 1H,  $J=7.5$  Hz, aromatic CH), 7.00 (d, 1H,  $J=7.99$  Hz, aromatic CH), 2.68 (t, 2H<sub>a</sub>,  $J=6.2$  Hz), 2.10-2.34 (m, 2H<sub>b</sub>), 1.93 (t, 2H<sub>c</sub>,  $J=6.0$  Hz).  $^{13}C$  NMR (100 MHz, DMSO- $d_6$ ):  $\delta$ (ppm) = 195.5, 178.5, 166.5, 159.0, 142.4, 135.0, 128.6, 123.6, 122.0, 117.8, 112.35, 109.6, 57.9, 47.3, 39.8, 27.2, 20.2.

#### 2'-Amino-2,5'-dioxo-5'H-spiro[indoline-3,4'-pyranol[3,2-c]chromene]-3'-carbonitrile (4b)

M.P: 289-293 (Lit. [49] 282-285 °C). FT-IR (KBr,  $cm^{-1}$ ): 3355, 3297, 3201, 3054, 2923, 2202, 1712, 1670, 1604, 1469, 1357, 1218, 1168, 1079, 975  $cm^{-1}$ .  $^1H$  NMR

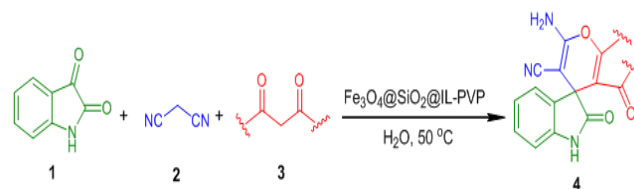
(400 MHz, DMSO- $d_6$ ):  $\delta$ (ppm)= 10.69 (s, 1H), 7.69 (s, 2H), 7.96 (d, 1H,  $J=7.6$  Hz aromatic CH), 7.84 (t, 1H,  $J=8$  Hz aromatic CH), 7.56 (t, 1H,  $J=7.7$  Hz aromatic CH), 7.50 (d, 1H,  $J=8.0$  Hz aromatic CH), 7.22-7.26 (m, 2H), 6.96 (t, 1H,  $J=7.6$  Hz aromatic CH), 6.88(d, 1H,  $J=8.0$  Hz aromatic)  $^{13}C$  NMR (100 MHz, DMSO- $d_6$ ):  $\delta$ (ppm)= 117.6, 158.8, 159.7, 155.5, 152.3, 142.6, 134.1, 133.5, 129.4, 125.5, 124.6, 123.1, 122.5, 117.4, 117.1, 112.9, 110.0, 101.9, 57.5, 48.1.

#### 2-Amino-7,7-dimethyl-2',5-dioxo-5,6,7,8-tetrahydrospiro[chromene-4,3'-indoline]-3-carbonitrile (4c)

M.P: 291-293 °C (Lit. [49]. 288-289 °C) FT-IR (KBr,  $cm^{-1}$ ): 3378, 3313, 3147, 2962, 2194, 1724, 1681, 1654, 1604, 1469, 1349, 1222, 1056, 902  $cm^{-1}$ .  $^1H$  NMR (400 MHz, DMSO- $d_6$ ):  $\delta$ (ppm)= 10.41 (s, 1H), 7.25 (s, 2H), 7.13-7.17 (m, 1H, aromatic CH), 7.00 (d, 1H,  $J=8.3$  Hz, aromatic CH), 6.90 (t, 1H,  $J=7.3$  Hz, CH<sub>2</sub>), 6.91 (d, 1H,  $J=7.94$  Hz, aromatic CH), 2.58 (s, 2H), 2.14 (s, 2H, CH<sub>2</sub>), 1.05 (s, 6H).  $^{13}C$  NMR (100 MHz, DMSO- $d_6$ ):  $\delta$ (ppm)= 195.36, 178.50, 164.62, 159.24, 142.53, 134.89, 128.64, 123.50, 122.15, 117.83, 111.26, 109.71, 57.93, 50.46, 47.28, 32.43, 28.08, 27.49.

#### 6'-amino-3'-methyl-2-oxo-1'-phenyl-1'H-spiro[indoline-3,4'-pyranol[2,3-c]pyrazole]-5'-carbonitrile (4e)

M.P: 235-238°C (Lit. [51]. 236-237°C). FT-IR (KBr,  $cm^{-1}$ ): 3459, 3297, 3174, 3073, 2923, 2194, 1700, 1654, 1519, 1465, 1392, 1330, 1218, 1126, 1068, 933, 752  $cm^{-1}$ .  $^1H$  NMR (400 MHz, DMSO- $d_6$ ):  $\delta$ (ppm)= 11.08 (s, 1H), 7.82 (d, 2H,  $J=3.8$  Hz CH), 7.62 (s, 2H, NH<sub>2</sub>), 7.54 (t, 2H,  $J=8.4$  Hz aromatic CH), 7.37 (t, 1H,  $J=8.4$  Hz aromatic CH), 7.31 (t, 1H,  $J=8.6$  Hz aromatic CH), 7.20 (d, 1H,  $J=3.5$  Hz aromatic CH), 6.99 (t, 1H  $J=8.2$  Hz aromatic CH), 7.00 (d, 1H,  $J=3.5$  Hz aromatic CH), 1.57 (s, 3H, me).  $^{13}C$  NMR (100 MHz, DMSO- $d_6$ ):  $\delta$ (ppm)= 178.01, 161.52, 145.42, 144.44, 142.08, 137.72, 132.62, 129.94, 129.77, 127.05, 125.39, 123.12, 120.61, 118.46, 110.33, 96.83, 56.64, 48.27, 19.04, 12.19.



**Scheme 2.** Synthesis of spirooxindole derivatives using a one-pot, three-component

### 3. Result and Discussion

$\text{Fe}_3\text{O}_4@\text{SiO}_2$  nanospheres core-shell is synthesized according to our previous work [46] and then 1-methyl-3-(3-trimethoxysilylpropyl)-1H-imidazole-3-ium chloride as an ionic liquid was synthesized from the reaction of (3-chloropropyl) trimethoxysilane with N-methyl imidazole at 80 °C. The as-prepared IL was grafted on the  $\text{Fe}_3\text{O}_4@\text{SiO}_2$  surface via the covalent interaction of the OH group of  $\text{Fe}_3\text{O}_4@\text{SiO}_2$  surface and the organosilane group of the ionic liquid. Finally, the polyvinyl pyrrolidone was reacted with IL on the  $\text{Fe}_3\text{O}_4@\text{SiO}_2$  by Coulomb force to obtain  $\text{Fe}_3\text{O}_4@\text{SiO}_2@\text{IL-PVP}$  catalyst. The physicochemical properties of  $\text{Fe}_3\text{O}_4@\text{SiO}_2@\text{IL-PVP}$  nanocatalyst were identified via XRD, FT-IR, SEM, TEM, TGA, VSM, and EDX.

In the FT-IR spectrum of  $\text{Fe}_3\text{O}_4@\text{SiO}_2@\text{IL-PVP}$  nanocatalyst (**Fig. 1a**), the appeared band at 3442  $\text{cm}^{-1}$  has corresponded to the characteristic absorption of the stretching O–H groups of  $\text{Fe}_3\text{O}_4$ . The intense broad absorption band at 1666  $\text{cm}^{-1}$  is belonged to the C=O group of N-vinylpyrrolidone as well as the stretching and bending vibrations of the C–H groups of N-vinylpyrrolidone be clear at 2938 and 1432  $\text{cm}^{-1}$ , respectively. The Si–O–Si and M (Fe and Si)-O stretching vibrations were appeared at 1093  $\text{cm}^{-1}$  and 576  $\text{cm}^{-1}$ , respectively.

The XRD pattern (**Fig. 1b**) was also performed to find out the crystallographic structure of the  $\text{Fe}_3\text{O}_4@\text{SiO}_2@\text{IL-PVP}$  which showed that the appearance diffraction peaks at  $2\theta=30.2^\circ$ ,  $35.5^\circ$ ,  $43.2^\circ$ ,  $53.6^\circ$ ,  $57^\circ$ , and  $62.4^\circ$  are satisfactory settlement with the standard XRD pattern of  $\text{Fe}_3\text{O}_4$ -NPs [47]. Also, the broadband at  $2\theta=10\text{--}16^\circ$  and  $20\text{--}25^\circ$  is related to the amorphous  $\text{SiO}_2$  and PVP, respectively. The finding confirms the high stability and well crystal ability of the  $\text{Fe}_3\text{O}_4$  NPs during modification processes.

The morphology of the  $\text{Fe}_3\text{O}_4@\text{SiO}_2@\text{IL-PVP}$  catalyst was studied using SEM (**Fig. 1c**) and TEM (**Fig. 1d**) images which possess the homogeneous morphology and roughly nanospherical particles in the range of 50–70 nm. Additionally, confirm the presence of spherical cores ( $\text{Fe}_3\text{O}_4$  NPs) and gray silica (organosilica) and PVP shell which revealed successful  $\text{Fe}_3\text{O}_4@\text{SiO}_2@\text{IL-PVP}$  formation.

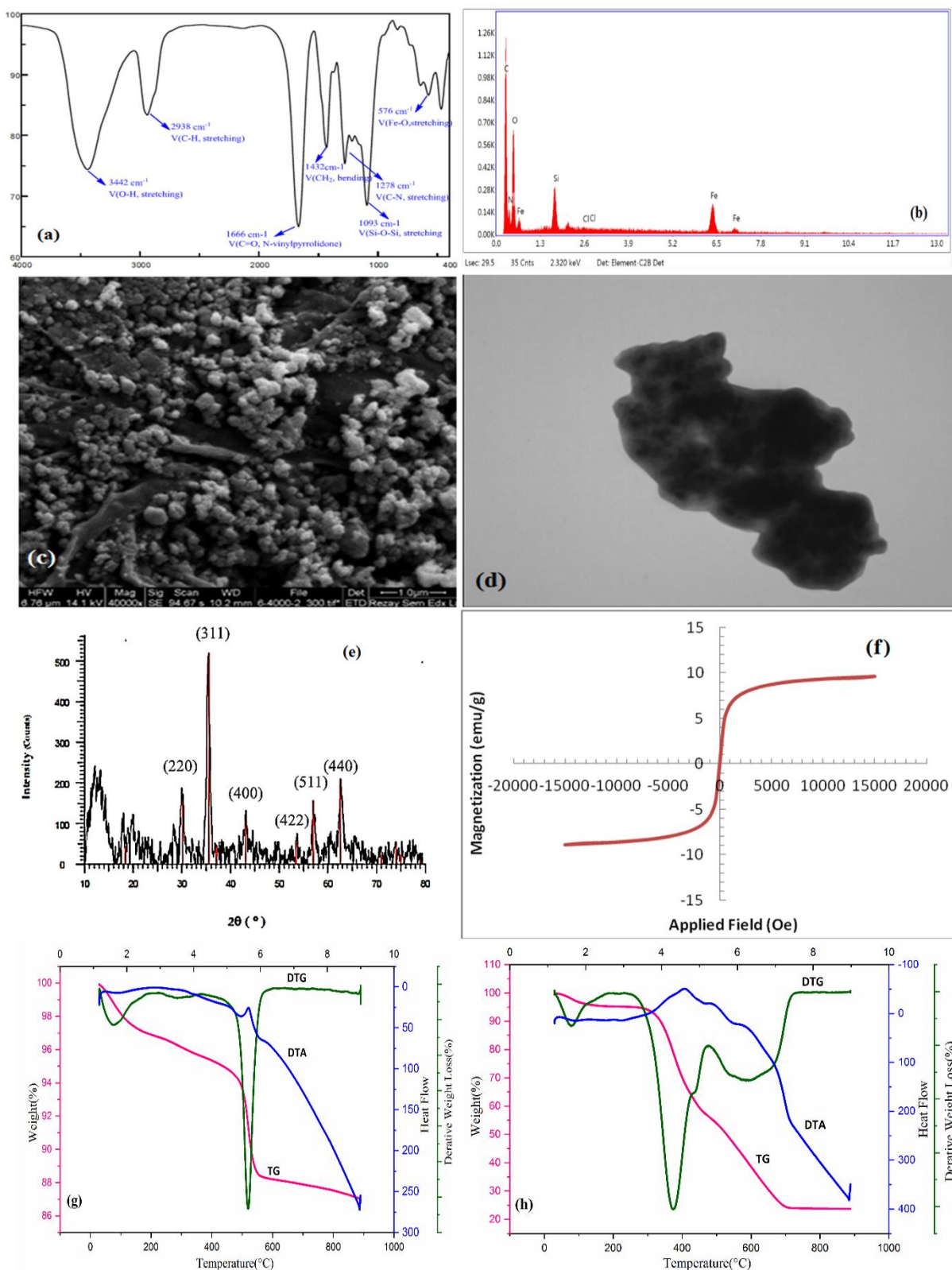
EDAX is utilized to signify the elemental composition (**Fig. 1e**) of the as-prepared catalyst and proved the exactness of Fe, O, Si, N, C, and Cl which revealed the successful synthesis of the desired catalyst.

The VSM analysis was utilized to investigate the magnetic character of the  $\text{Fe}_3\text{O}_4@\text{SiO}_2@\text{IL-PVP}$  catalyst (**Fig. 1f**). As seen, the saturation magnetization of  $\text{Fe}_3\text{O}_4$  after silica, IL, and polyvinylpyrrolidone

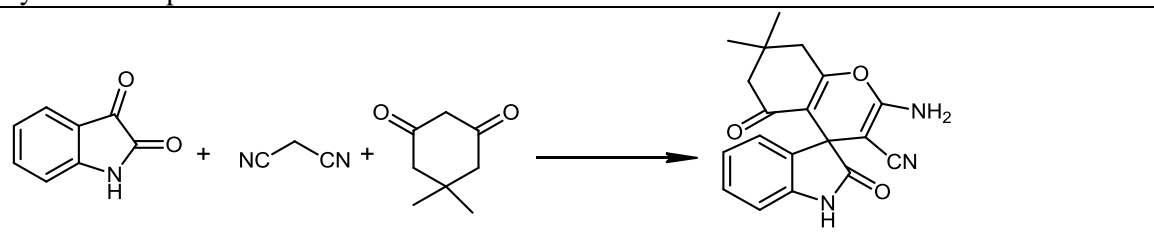
modifying decreased which is due to the surface effects and the different crystallinity structures of other materials.

In the next step, the thermochemical behavior and stability of the as-prepared catalyst were studied by TGA which was conducted in an  $\text{N}_2$  atmosphere in the range of 30 to 800 °C (**Fig. 1g**). As seen that after adding the PVP,  $\text{Fe}_3\text{O}_4@\text{SiO}_2@\text{IL}$  has become much more stable. Additionally, the TGA curve of the  $\text{Fe}_3\text{O}_4@\text{SiO}_2@\text{IL}$  revealed two diminishing weights the first emerges peak at a temperature before 140 °C owing to the desorption of surface adsorbed  $\text{H}_2\text{O}$ . This is pursuing by appearance peak at 380–620 °C which corresponded to the decay of existing organic materials. The founding confirms the presence of the ILs on the  $\text{Fe}_3\text{O}_4@\text{SiO}_2$  surface (**Fig. 1g**). The  $\text{Fe}_3\text{O}_4@\text{SiO}_2@\text{IL-PVP}$  TGA curve showed a weight loss (below 100 °C) which is able to attribute to the water leaching and surface OH groups. The second weight loss (20%) at 250 to 370 °C is related to the degradation of IL groups and the other weight loss between 480 to 600 °C is attributed to the dissociation of the PVP and other organic structure. As a result, it can be claimed that the  $\text{Fe}_3\text{O}_4@\text{SiO}_2@\text{IL-PVP}$  was fully stable up to 250 °C and confirms that it may perhaps be cautiously utilized in similar reactions up to approximately 200 °C.

Due to the capability of  $\text{Fe}_3\text{O}_4@\text{SiO}_2@\text{IL-PVP}$  as a mild and robust acidic catalyst, typically its catalytic capability has been studied for the preparation of the spirooxindole derivatives (See **Scheme 2**). Therefore, at the first step operational parameters (catalyst mass, solvent type, reaction temperature, and reaction time) were optimized to achieve the highest efficiency. Initially, in the lack of organic and water solvent, a typical reaction was conducted by condensation of isatin (1 mmol) with dimedone (1 mmol), and malononitrile (1 mmol) in the existent of different  $\text{Fe}_3\text{O}_4@\text{SiO}_2@\text{IL-PVP}$  amounts at 50 °C (See **Table 1**). Finding confirm that in the absence of the catalyst exclusively a slight product mass has been obtained even after the extended time (See **Table 1**, entries 1 and 2). Although at 0.01 g of the  $\text{Fe}_3\text{O}_4@\text{SiO}_2@\text{IL-PVP}$  catalyst excellent yield (95%) was achieved in a short reaction time (15 min) which is due to the accessibility of more functional catalytic locations (See **Table 1**, entry 4). Higher  $\text{Fe}_3\text{O}_4@\text{SiO}_2@\text{IL-PVP}$  mass did not improve the efficiency or reaction time significantly which can be said that with increasing  $\text{Fe}_3\text{O}_4@\text{SiO}_2@\text{IL-PVP}$  dosage, the reacting molecules become as far apart as possible and access to the reacting groups becomes more difficult (**Table 1**, entry 5). As well, an excessive amount of  $\text{Fe}_3\text{O}_4@\text{SiO}_2@\text{IL-PVP}$  catalyst can increase the reaction rate and cause byproduct (tarry substances)



**Fig. 1** (a) The FT-IR spectra, (b) Energy-dispersive X-ray spectroscopy (EDX) spectra, (c) Scanning electron microscope (SEM) image, (d) Transmission electron microscopy (TEM) image, (e) X-ray diffraction patterns (XRD), (f) Vibrating sample magnetometer (VSM) of  $\text{Fe}_3\text{O}_4@SiO_2@IL-PVP$ , (g) Thermal gravimetric analysis (TGA) of  $\text{Fe}_3\text{O}_4@SiO_2@IL$  and (h) Thermal gravimetric analysis (TGA) of  $\text{Fe}_3\text{O}_4@SiO_2@IL-PVP$ .

**Table 1.** Optimization of the amount of catalyst, solvent and the reaction temperature for the synthesis of spirooxindoles


Entry	Catalyst (g)	Solvent	Temperature (°C)	Time (min.)	Yield <sup>a</sup> (%)
1	-	-	50	360	<10
2	-	H <sub>2</sub> O	50	190	15
3	0.005	H <sub>2</sub> O	50	40	86
4	0.01	H <sub>2</sub> O	50	15	95
5	0.015	H <sub>2</sub> O	50	12	92
6	0.01	H <sub>2</sub> O	25	90	65
7	0.01	H <sub>2</sub> O	40	45	80
8	0.01	H <sub>2</sub> O	60	25	88
9	0.01	H <sub>2</sub> O	80	35	85
10	0.01	-	50	130	35
11	0.01	EtOH	50	80	75
12	0.01	MeOH	50	40	85
13	0.01	MeCN	50	240	25

<sup>a</sup> Isolated yield

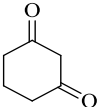
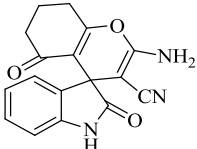
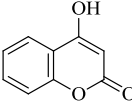
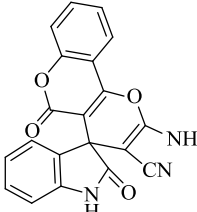
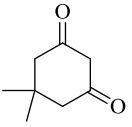
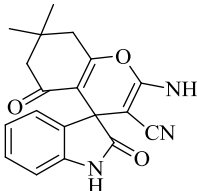
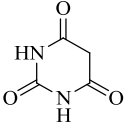
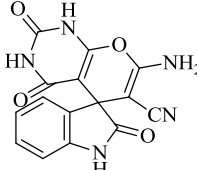
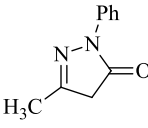
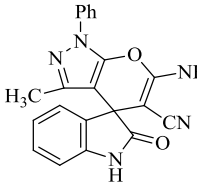
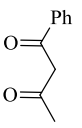
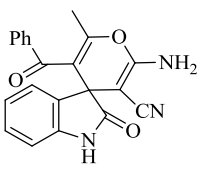
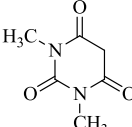
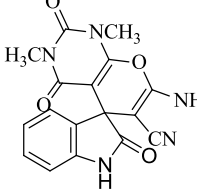

formation or decomposition of main products which can be deposit on the catalyst and may be causing a decrease in catalyst activity or they may be acting as poisons and decreasing catalyst activity. To compare the capability of the solvent conditions against the solvent-free method, different experiments were performed on the model reaction catalyzed with Fe<sub>3</sub>O<sub>4</sub>@SiO<sub>2</sub>@IL-PVP (0.01 g) in numerous solvents such as distilled water, acetonitrile, methanol, and ethanol under heating conditions (50°C) (**Table 1**). The finding revealed that the short reaction time superior efficiencies of the product were achieved in water media. Also, the model reaction has been tested in solvent-free conditions at 50 °C which provided a production efficiency of 35 % after 130 min (See **Table 1**, entry 10).

To confirm the capability of the as-prepared catalyst in optimizing conditions, the preparation of spiro-oxindole derivatives (4a-4j) was conducted in the presence of heterogeneous and recoverable Fe<sub>3</sub>O<sub>4</sub>@SiO<sub>2</sub>@IL-PVP nanocatalyst. The finding revealed that in all samples the correlated spirooxindoles were achieved in satisfactory to fine yields in desirable time (**Table 2**, entries 1-10). The multistage as-designed mechanism for the preparation of spirooxindoles (**Scheme 3**) revealed that in the first stage, the proton the existing ionic liquid interact with the O atom of the C=O group of the isatin probably via the H-bond generation, as an outcome of intensifying the electrophilic properties of

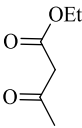
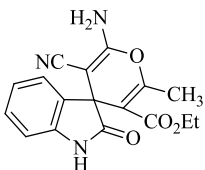
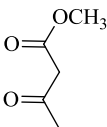
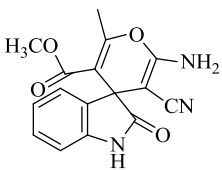
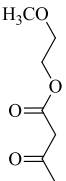
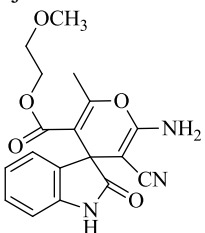
the aldehyde C=O group [48]. Knoevenagel condensation of isatin with malononitrile takes place to afford isatylidene malononitrile derivative (**I**) and then, this intermediate as a Michael addition attacked of 1,3-diketone to provide the intermediate (**II**) or (**III**) resulted by the cycloaddition of the OH group to the cyano moiety to generate the demanded products (**IV**) and (**V**).

To evaluate the efficiency of as-prepared catalyst and methodology, this strategy was compared with reported catalysts in the reaction of understudy species (**Table 3**). As seen, it is clear that the suggested methodology with Fe<sub>3</sub>O<sub>4</sub>@SiO<sub>2</sub>@IL-PVP NPs (as a robust eco-friendly catalyst) is superior to other methods concerning the duration of reaction, yields of products, mild reaction conditions, and solvents type. From an organic and phytochemistry vision, the use of a green magnetite-based heterogeneous catalyst owing several advantages including simple catalyst separability, recoverability, and recyclability is an appropriate solution to improve the efficiency of organic reactions. The possibility of the durability of the as-prepared catalyst was studied by using a model reaction medium containing isatin, malononitrile, dimedone and Fe<sub>3</sub>O<sub>4</sub>@SiO<sub>2</sub>@IL-PVP (0.01 g) at 50 °C in distilled water. Finally, the Fe<sub>3</sub>O<sub>4</sub>@SiO<sub>2</sub>@IL-PVP catalyst has been separated and collected from the reaction media and soaked in hot ethanol several times, then dried at 80 °C for future

**Table 2.** Preparation of spirooxindoles 4 in the presence of Fe<sub>3</sub>O<sub>4</sub>@SiO<sub>2</sub>@IL-PVP<sup>a</sup>

Entry	1,3-dicarbonyl compounds	Product	Time (min)	Yield <sup>b</sup> (%)	Mp <sup>c</sup> .(°C) (Lit)
1		4a 	5	96	300-302 (298-299) <sup>[49]</sup>
2		4b 	15	93	289-293 (284-286) <sup>[50]</sup>
3		4c 	15	95	291-293(288-289) <sup>[50]</sup>
4		4d 	45	85	272-275(271-274) <sup>[51]</sup>
5		4e 	30	90	235-238(236-237) <sup>[52]</sup>
6		4f 	70	77	263-265(261-263) <sup>[40]</sup>
7		4g 	25	88	230-232(231-233) <sup>[53]</sup>
		4h 			

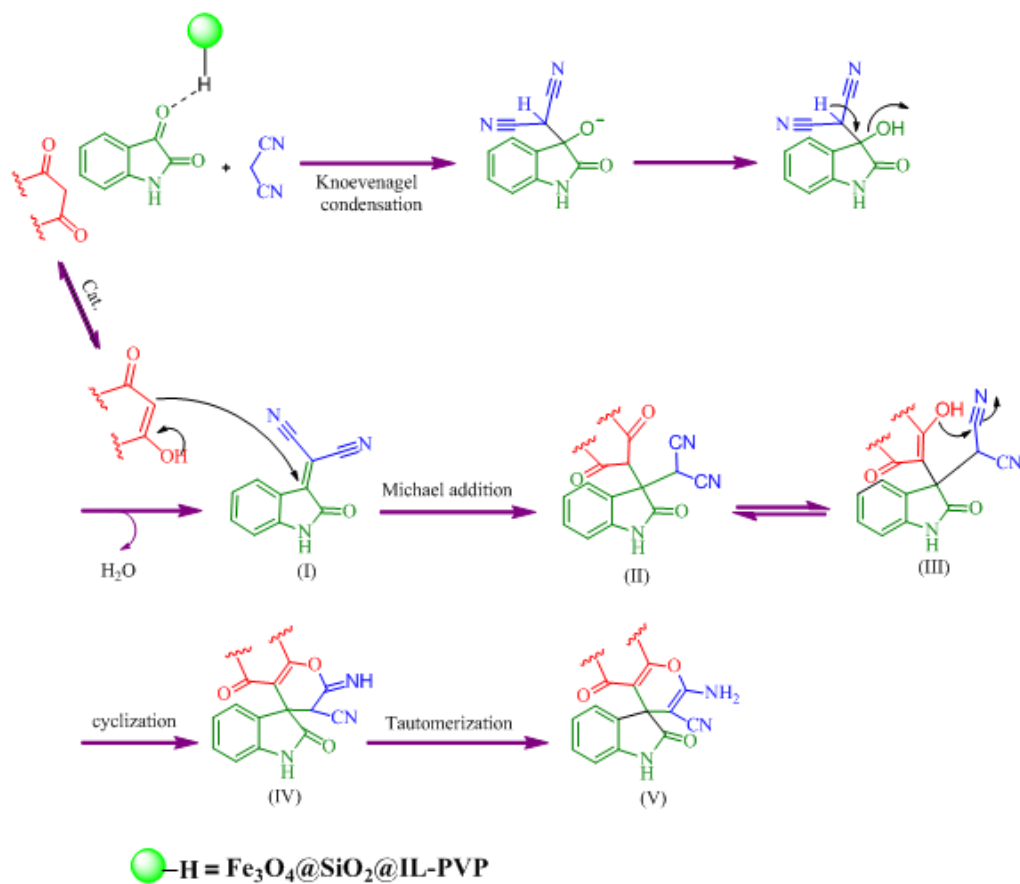


8			30	80	257-260(255-256) <sup>[40]</sup>
9			45	75	283-285(280-281) <sup>[53]</sup>
10			25	82	180-184(179-181) <sup>[54]</sup>

<sup>a</sup>Reaction conditions: isatin = 1 mmol, 1,3-dicarbonyl compounds = 1 mmol, malononitrile = 1 mmol, Fe<sub>3</sub>O<sub>4</sub>@SiO<sub>2</sub>@IL-PVP = 0.01 g

<sup>b</sup>Isolated yield

<sup>c</sup>Melting points are uncorrected



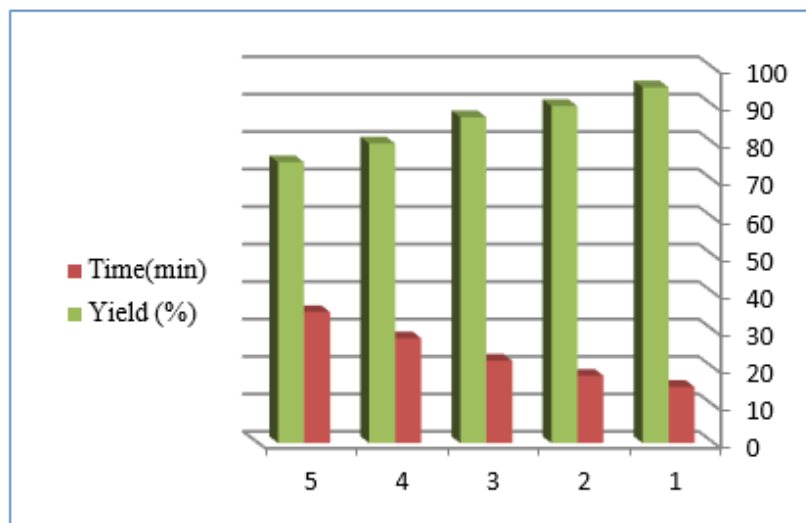
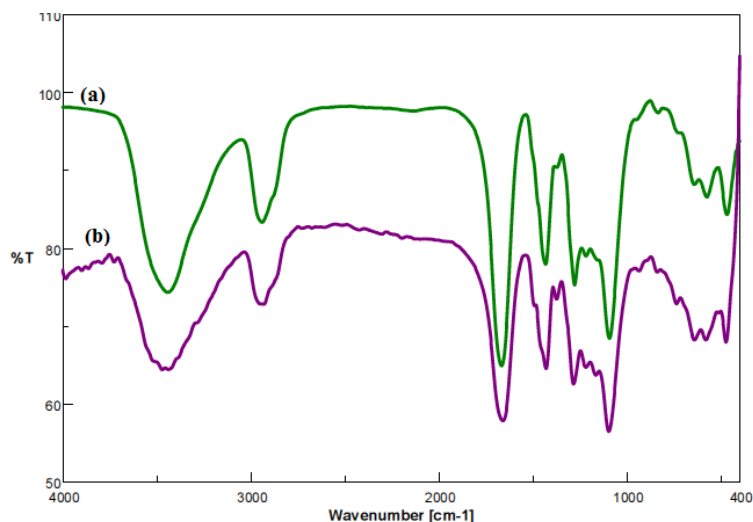
**Scheme 3.** A plausible mechanism for synthesis of spirooxindoles 4a-4q in the presence of Fe<sub>3</sub>O<sub>4</sub>@SiO<sub>2</sub>@IL-PVP

**Table 3.** Comparison of the efficiency of Fe<sub>3</sub>O<sub>4</sub>@SiO<sub>2</sub>@IL-PVP NPs with other catalysts for the synthesis of 4a

Entry	Catalyst	Conditions	Time (min)	Yield (%)	References
1	Citric acid	H <sub>2</sub> O/EtOH(2:1), 80°C	10	81	[44]
2	Sodium stearate	H <sub>2</sub> O, 60°C	180	95	[41]
3	TEBA	H <sub>2</sub> O, 60°C	180	90	[39]
4	InCl <sub>3</sub>	CH <sub>3</sub> CN, Reflux	90	75	[35]
5	β-cyclodextrine	H <sub>2</sub> O, 60°C	300	90	[37]
6	Fe <sub>3</sub> O <sub>4</sub> @SiO <sub>2</sub> -imid-PMA	H <sub>2</sub> O, 60°C	90	93	[45]
7	ZnFe <sub>2</sub> O <sub>4</sub>	H <sub>2</sub> O, 100°C	8	86	[55]
8	SBA-Pr-NH <sub>2</sub>	H <sub>2</sub> O, Reflux	5	91	[42]
9	TBAF	H <sub>2</sub> O, Reflux	30	97	[36]
10	Fe <sub>3</sub> O <sub>4</sub> @SiO <sub>2</sub> @IL-PVP	H <sub>2</sub> O, 50°C	15	95	This Work

experiments. Findings revealed that the catalyst is able to recover and reused in five reaction cycles with a negligible decline in the reaction efficiency (See **Fig. 2**). The FT-IR spectrum of the recovered Fe<sub>3</sub>O<sub>4</sub>@SiO<sub>2</sub>@IL-PVP nanocatalyst was also carried out to evaluate the durability of PVP and IL moieties during the reaction

process and the result was compared with the fresh Fe<sub>3</sub>O<sub>4</sub>@SiO<sub>2</sub>@IL-PVP nanocatalyst (**Fig. 3**). The FT-IR spectrum of the as-applied Fe<sub>3</sub>O<sub>4</sub>@SiO<sub>2</sub>@IL-PVP catalyst after five cycles is very close to that of the fresh catalyst and confirms the chemical stability and durability of the catalyst overall the recycling steps.

**Fig. 2** Recyclability of Fe<sub>3</sub>O<sub>4</sub>@SiO<sub>2</sub>@IL-PVP a catalyst in the condensation reaction of isatin, malononitrile, and dimedone**Fig. 3** FT-IR spectra for the comparison of fresh catalyst (a) and recycled catalyst after five times (b).

#### 4. Conclusions

Herein, an environmentally friendly and robust strategy was utilized for the synthesis of the spiroxindole derivatives catalyzed by as-designed and prepared  $\text{Fe}_3\text{O}_4@\text{SiO}_2@\text{IL-PVP}$  nanocatalyst in aqueous media. In addition, the as-prepared  $\text{Fe}_3\text{O}_4@\text{SiO}_2@\text{IL-PVP}$  catalyst is able to be readily collected by using an external magnet from reaction media and re-applied in the proposed system without any considerable deprivation of catalytic activity after five runs which represent a consequential benefit for organic reactions from an environmental and economic vision.

#### Acknowledgments

The authors gratefully acknowledge partial support of this work by Yasouj University, Yasouj, Iran

#### References

- [1] A. Ghorbani-Choghamarani, M. Norouzi, *Appl. Organometal. Chem.* 30 (2016) 140–147.
- [2] J. Davarpanah, S. Elahi, P. Rezaee, *J. Porous Mater.* 25 (2018) 161–170.
- [3] G. Azadi, A. Ghorbani-Choghamarani, *Appl. Organometal. Chem.* 30 (2016) 360–366
- [4] J. Davarpanah, A. R. Kiasat, *Catal. Commun.* 42 (2013) 98–103.
- [5] A. Ghorbani-Choghamarani, G. Azadi, *RSC Adv.* 5 (2015) 9752–9758.
- [6] M. A. Zolfigol, V. Khakyzadeh, A. R. Moosavi-Zare, A. Rostami, A. Zare, N. Iranpoor, M. H. Beyzavid, R. Luque, *Green Chem.* 15(2013) 2132–2140.
- [7] B. Atashkar, A. Rostami, B. Tahmasbi, *Catal. Sci. Technol.* 3 (2013) 2140–2146.
- [8] L. Shiri, A. Ghorbani-Choghamarani, M. Kazemi, *Res. Chem. Intermed.* 43 (2017) 2707–2724
- [9] S. Rayati, F. Nejabat, S. Zakavi, *Inorg. Chem. Commun.*, 40 (2014) 82–86.
- [10] A. Rostami, B. Tahmasbi, F. Abedi, Z. Shokria, *J. Mol. Catal. A: Chem.* 378 (2013) 200–205
- [11] W. Wu, Q. He, C. Jiang, *Nanoscale Res. Lett.* 3 (2008) 397–415.
- [12] M. Esmailpour, J. Javidi, F. Nowroozi-Dodeji, M. Mokhtari-Abarghousi, *Transition Met. Chem.* 39 (2014) 797–809.
- [13] A. Kong, P. Wang, H. Zhang, F. Yang, S. P. Huang, Y. Shan, *Appl. Catal. A: Gen.* 417 (2012) 183–189.
- [14] D. K. Kim, M. Mikhaylova, F. H. Wang, J. Kehr, B. Bjelke, Y. Zhang, M. Muhammed, *Chem. Mater.* 15 (2003) 4343–4351.
- [15] L. F. Gamarra, G. E. S. Brito, W. M. Pontuschka, E. Amaro, A. H. C. Parma, G. F. Goya, *J. Magn. Magn. Mater.* 289 (2005) 439–441.
- [16] E. H. Kim, H. S. Lee, B. K. Kwak, B. K. Kim, *J. Magn. Magn. Mater.* 289 (2005) 328–330.
- [17] N. Kohler, G. E. Fryxell, M. Zhang, *J. Am. Chem. Soc.* 126 (2004) 7206–7211.
- [18] B. Schöpf, T. Neuberger, K. Schulze, A. Petri, M. Chastellain, M. Hofmann, H. Hofmann, B. Von Rechenberg, *J. Magn. Magn. Mater.* 293 (2005) 411–418.
- [19] M. Iijima, Y. Yonemochi, M. Tsukada, H. Kamiya, *J. Colloid Interface Sci.* 298 (2006) 202–208.
- [20] Y. Zhang, J. Y. Liu, S. Ma, Y. J. Zhang, X. Zhao, X. D. Zhang, Z. D.; Zhang, *J. Mater. Sci. Mater. Med.* 21 (2010) 1205–1210.
- [21] M. Faraji, Y. Yamini, M. Rezaee, *J. Iran. Chem. Soc.* 7 (2010) 1–37.
- [22] a) M. Benaglia, A. Puglisi, F. Cozzi, *Chem. Rev.* 103 (2003) 3401–3430.; b) F. Cozzi, *Adv. Synth. Catal.* 348 (2006) 1367–1390.
- [23] S. M. Baghbanian, N. Rezaeia, H. Tashakkorian, *Green Chem.* 15 (2013) 3446–3458.
- [24] R. S. Priya, P. Karthikeyan, *Mater. Today Chem.* 1 (2016) 46–51.
- [25] A. R. Kiasat, J. Davarpanah, *J. Mol. Catal. A: Chem.* 373 (2013) 46–54.
- [26] H. R. Shaterian, M. Ghashang, M. Feyzi, *Appl. Catal. A: Gen.* 2 (2008) 128–33.
- [27] K. Ding, Y. Lu, Z. Nikolovska-Coleska, S. Qiu, Y. Ding, W. Gao, J. Stuckey, K. Krajewski, P. P. Roller, Y. Tomita, D. A. Parrish, *J. Am. Chem. Soc.* 29 (2005) 10130–10131.
- [28] B. K. S. Yeung, B. Zou, M. Rottmann, S. B. Lakshminarayana, S. H. Ang, S. Y. Leong, J. Tan, J. Wong, S. Keller-Maerki, C. Fischli, A. Goh, E. K. Schmitt, P. Krastel, E. Francotte, K. Kuhen, D. Plouffe, K. Henson, T. Wagner, E. A. Winzeler, F. Petersen, B. Reto, V. Dartois, T. Diagana, T. H. T. Keller. *J. Med. Chem.* 14 (2010) 5155–5164.
- [29] K. Lundahl, J. Schut, J. L. M. A. Schlatmann, G. B. Paerels, and A. Peters. *J. Med. Chem.* 2 (1972) 129–132.
- [30] A. Thangamani, *Eur. J. Med. Chem.* 12 (2010) 6120–6126.
- [31] A. J. Kell, D. L. B. Stringle, M. S. Workentin, *Org. Lett.* 2 (2000) 3381–3384.
- [32] K. C. Nicolaou, S. Sanchini, D. Sarlah, G. Lu, T. R. Wu, D. K. Nomura, B. F. Cravatt, B. Cubitt, J. C. de la Torre, A. J. Hessell, D. R. Burton, *Proc. Natl. Acad. Sci. U.S.A.* 108 (2011) 6715–6720.
- [33] P. Prasanna, K. Balamurugan, S. Perumal, P. Yogeewari, D. Sriram, *Eur. J. Med. Chem.* 45 (2010) 5653–5661.

- [34] A. Nandakumar, P. Thirumurugan, P.T. Perumal, P. Vembu, M.N. Ponnuswamy, P. Ramesh, *Bioorg. Med. Chem. Lett.* 20 (2010) 4252-4258.
- [35] G. Shanthi, G. Subbulakshmi, P. T. Perumal, *Tetrahedron* 63 (2007) 2057-2063.
- [36] S. Gao, C. H. Tsai, C. Tseng, C. F. Yao. *Tetrahedron*.64 (2008) 9143-9149.
- [37] R. Sridhar, B. Srinivas, B. Madhav, V. P. Reddy, Y. V. D. Nageswar, K. R.Rao, *Can. J. Chem.* 87 (2009) 1704-1707.
- [38] M. Dabiri, M. Bahramnejad, M. Baghbanzadeh. *Tetrahedron*. 65 (2009) 9443-9447.
- [39] S. L. Zhu, S. J. Ji, Y. Zhang. *Tetrahedron*. 63 (2007) 9365-9372.
- [40] G. S. Hari, Y. R. Lee. *Synthesis*.3 (2010) 453-464.
- [41] L. M. Wang, N. Jiao, J. Qiu, J. J. Yu, J. Q. Liu, F. L. Guo, Y. Lu, *Tetrahedron*. 66 (2010) 339-343.
- [42] Gh. Mohammadiziarani, A. Badiei, S. Mousavi, N. Lashgari, A. Shahbazi, *Chin. J. Catal.* 33 (2012) 1832-1839.
- [43] A. R. Hasaninejad, N. Golzar, M. Beyrati, A. Zare, M. M. Doroodmand, *J. Mol. Catal. A. Chem.* 372 (2013) 137-150.
- [44] Z. Karimi, A. H. Fereydoonzhad, *Iran. Chem. Commun.* 5 (2017) 407-416.
- [45] M. Esmaeilpour, J. Javidi, M. Divar, *J. Magn. Mater.* 423 (2017) 232-240.
- [46] Sh. Vaysipour, M. Nasr-Esfahani, Z. Rafiee, *Appl. Org. Chem.* 33 (2019) 1-11.
- [47] N. Azgomi, M. Mokhtary, *J. Mol. Catal. A: Chem.* 398 (2015) 58-64.
- [48] C. Garkoti, J. Shabir, S. Mozumdar, *New J. Chem.* 41 (2017) 9291-9298.
- [49] Y. Li, H. Chen, Ch. Shi, D. Shi, Sh. Ji, *J. Comb. Chem.* 12 (2010) 231-237.
- [50] M. Kidwai, A. Jahan, N.K. Mishra, *Appl. Catal. A Gen.* 425 (2012) 35-43.
- [51] Z. Karimi Jaber, *Iran. Chem. Commun.*, 5 (2017) 407-416.
- [52] M. N. Elinson, A. S. Dorofeev, F. M. Miloserdov, G. I. Nikishin, *Mol. Divers.* 13 (2009) 47-52.
- [53] R. Jamatia, A. Gupta, A. K. Pal, *RSC. Adv.*, 6 (2016) 20994-21000.
- [54] G. D. Wang, X. N. Zhang, Z. H. Zhang, *J. Heterocycl. Chem.* 50 (2013) 61-65.
- [55] H. Hasani, M. Irizeh, *Asian J. Green Chem.* 2 (2018) 85-95.